Received March 3, 2018, accepted April 2, 2018, date of publication April 11, 2018, date of current version June 5, 2018.

Digital Object Identifier 10.1109/ACCESS.2018.2825607

Automatic Characterization System of Switched Reluctance Machines and Nonlinear Modeling by Interpolation Using Smoothing Splines

TÁRCIO ANDRÉ DOS SANTOS BARROS[1], (Member, IEEE), PEDRO JOSÉ DOS SANTOS NETO[2], (Student Member, IEEE), MARCELO VINICIUS DE PAULA[2], (Student Member, IEEE), ADSON BEZERRA MOREIRA[3], (Member, IEEE), PAULO SERGIO NASCIMENTO FILHO[2], AND ERNESTO RUPPERT FILHO[2], (Member, IEEE)

[1]Faculty of Mechanical Engineering, University of Campinas, Campinas-SP 13083-740, Brazil
[2]Faculty of Electrical and Computer Engineering, University of Campinas, Campinas-SP 13083-740, Brazil
[3]Department of Electrical Engineering, Federal University of Ceará, Sobral-CE 62010-560, Brazil

Corresponding author: Tárcio André Dos Santos Barros (tarcioandre@hotmail.com)

This work was supported by the São Paulo Research Foundation, FAPESP under Grant 2017/21640-9, Grant 15/03248-9, and Grant 16/08645-9.

ABSTRACT This paper presents a high resolution automatic system capable of performing magnetic characterization tests and obtaining the data needed to conduct reliable models for switched reluctance machines (SRM). In addition, the detailed description of the instrumentation system performed in this paper has as contribution the study of mathematical interpolation techniques for the treatment process of test data to obtain a nonlinear model based on lookup tables. It was observed that the commonly used polynomial regressions may cause inaccuracies in the final characteristics of the model data. Thereat, smoothing splines were applied, which results in more accurate and consistent results for the SRMs operation. Thus, it is possible to obtain control projects, optimization systems and advanced studies through computer simulations. Simulation and experimental results have proved the efficiency of the system and have confirmed the importance of achieving real curves when accurate models of a SRM are needed.

INDEX TERMS Switched reluctance machine, magnetization curves, smoothing splines.

I. INTRODUCTION

Switched Reluctance Machine(SRM) is a double salient machine (rotor and stator) which has field coils in the stator slots and has no coils or magnets in its rotor. The rotor consists of ferromagnetic materials with regular protrusions [1]. In Fig. 1 it is depicted a SRM 12/8 (number of stator poles/number of rotor poles).

The SRM operation principle as a motor is based on the principle of minimum reluctance, i.e., when the winding on a pair of stator poles is energized, the poles of the rotor are attracted to a position representing the minimum reluctance (aligned axes), generating torque on the rotor [1]–[3]. Due to the characteristics such as mechanical strength, high starting torque, high efficiency and low manufacturing cost, SRM has become a strong candidate for applications where one wants to work at a variable speed either as motor or generator. Among its main applications are the use of SRM in electric vehicles, wind power generation and driving oil pumps [4]–[10]. The main impediments to the use of SRM are torsional oscillations, audible noise and need of position sensors. There are a lot of efforts to increase the performance of SRM and for mitigation of these obstacles [11]–[13].

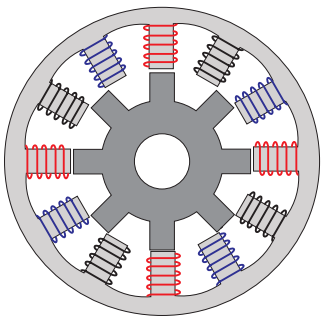

FIGURE 1. Representation of a SRM 12/8 poles.

The existence of double salience and the fact that they usually operate in the region of magnetic saturation imply that SRMs have highly nonlinear characteristics that hinder the project and development of controls; since it is not possible to represent the SRM by an efficient linear model as it is done for the induction machine and synchronous machine [14]. Several nonlinear models have been studied and tested and are of fundamental importance to enable studies of new control techniques, projects and estimation of SRM speed [14]–[16]. Because the simulation efficiency is entirely related to the accuracy of the mathematical model, the mathematical model must accurately depict the magnitudes behavior of the system to be simulated.

Magnetic flux (Φ), electric current (I) and the rotor position (θ) are directly related one to each other. Thus, modeling the SRM electrical and mechanical behavior is necessary to obtain the magnetization curves $\Phi(I,\theta)$ [17], [18]. In [19]–[21] methods are presented to obtain the magnetization curves quickly from a few experimental tests. These methods are recommended for application where it is not possible to couple the rotor with brakes. However, these methods have lower accuracy than the method of blocking the rotor at various positions [22].

With the magnetization curves $\Phi(I,\theta)$ obtained experimentally, lookup tables and artificial neural network are generally used to build models for SRM [14], [22]. A high number of data are required to perform these models [19]. The number of curves obtained by experimental testing is limited by the accuracy and the test execution time. Therefore, a mathematical processing is generally used to achieve a larger number of magnetization curves. In [23]–[25] analytical equations are developed to obtain intermediary magnetization curves. On the other hand, experimental process errors (sensors error measuring, noises, residual flows, numerical integrations) are present in the data obtained experimentally in magnetization tests [22], [26]. These errors can result in an inconsistent characteristics of SRM operation. Thus, the mathematical processing to get the lookup tables for current $I(\Phi,\theta)$ and electromagnetic torque $T(I,\theta)$ must be robust to these errors.

This article presents an automatic system that allows to obtain the magnetization curves of switched reluctance machines. It was observed that the commonly used polynomial regressions can cause inaccuracies in the final characteristics of the model data. Moreover, smoothing splines technique allows to obtain a more accurate and consistent model. Finally, simulation and experimental results have proved the efficiency of the system and have confirmed the importance of achieving real curves when accurate models of a SRM are needed.

II. NONLINEAR CHARACTERISTICS OF SRM

The magnetization curves $\Phi(I,\theta)$ are highly nonlinear because SRM operates mainly in the saturation region. These curves can be obtained mainly in three ways: calculated by finite element, analytical approximations and experimental measurements. When one has the characteristics and physical dimensions of SRM, it is possible to use the finite elements method to calculate the magnetization curves. The need for these data makes this method difficult to perform in cases that one do not have the data from the machine project design [27]–[29]. If the objective is to design the converter, verify basic control systems or when only SRM basic data are available, it is appropriate to determine the magnetization curves through analytical expressions. Some functions that calculate the SRM magnetization curves approximately are presented in [30]and [31].

More precise SRM magnetization curves, which allow obtaining more reliable models, can be obtained by means of experimental tests. In these tests, magnetization curves are obtained for different rotor positions. Direct or indirect methods can be applied to determine the SRM magnetization curves experimentally. The indirect method consists basically in determining the magnetization curves from the static torque. This method is extremely complicated to be performed with good accuracy, since any mechanical deviation leads to large errors. Direct methods consist in applying voltages in the SRM phases and determine the magnetic flux. One way of obtaining the magnetization curves consists in applying a sinusoidal alternating voltage in the motor winding pair for several positions. Thus, knowing the resulting RMS current, winding resistance and the drop voltage and current, it is possible to determine the flux linkage. This method introduces errors if magnetic saturation occurs, a fact that usually happens with SRM. Another way to calculate the flow is through the rise and fall time of the current transient, as done in [32].

The most widely used test consists in blocking the rotor and applying a voltage step for each rotor position, storing current and voltage data. Knowing the stage of resistance, then it is possible to determine the flux linkage through Eq.(1).

$$\phi_j(t) = \int_0^t (V_j - R_j I_j)dt \tag{1}$$

This method was performed in this work because it presents better results as discussed in [14]. However, as a novel contribution, an automatic system was developed to obtain the magnetization curves accurately and for a sufficient number of locations to represent the SRM accurately.

III. AUTOMATIC SYSTEM DESIGNED TO PERFORM SRM TEST

To perform the SRM characterization test, an experimental configuration was assembled, as shown in Fig. 2. The magnetization test consists in placing the machine rotor automatically at known positions and applying a voltage step to obtain the transient response of the SRM phase current. To position the rotor shaft automatically, a stepper motor was used along with a drive with micro steps (with maximum resolution of 40000 steps per revolution).

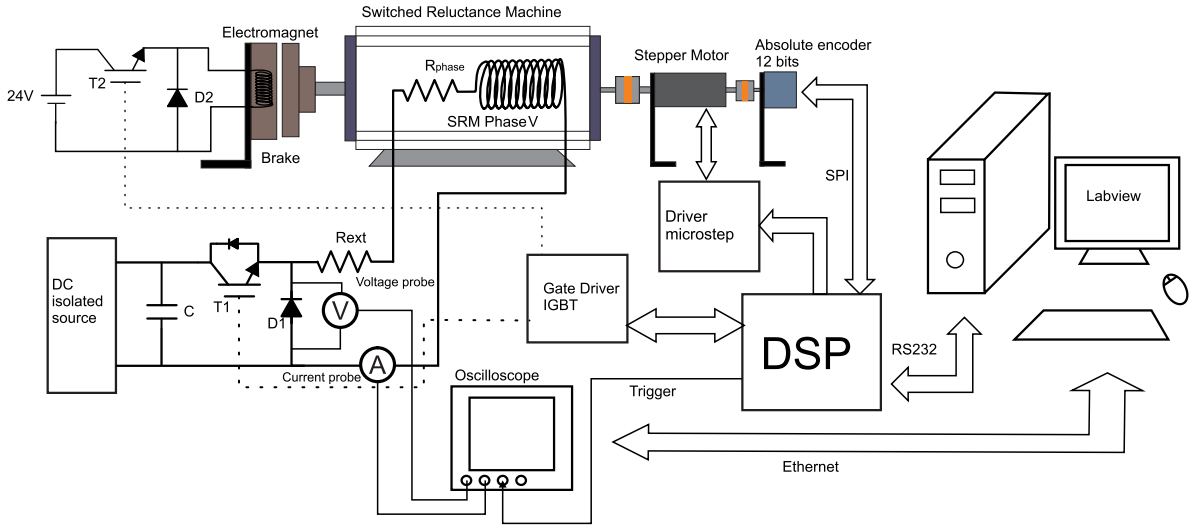

FIGURE 2. General diagram of the automated system to obtain the magnetization curves.

A digital signal processor (DSP) (TMS320F28335-*Texas Instruments*) is responsible for managing the positioning control of the rotor shaft. By means of an absolute encoder (RE36SC06H2B-*Renishaw*), which has 12-bit resolution (0.087 degrees), the DSP obtains the position of the rotor shaft and adjusts the desired position by sending pulses to the stepper motor drive. When the rotor shaft is in the desired position, an electromechanical brake, which is connected to the rotor shaft, is driven by the DSP in order to lock the shaft. To apply the voltage step in the SRM, a phase drive circuit was implemented to be tested. The voltage step is applied to the machine throughout a command coming from the DSP. The voltage and the current in the winding phase under test are obtained by an oscilloscope (Lecroy® 24MXs-B) using current and voltage high resolution isolated probes.

For the test control and automatic management, an interface software in *LabView* was developed to communicate with the DSP via serial communication (RS-232) and with the oscilloscope via Ethernet (IP protocol). Fig. 3 shows the flowchart of the program developed in LabView. Initially, the program obtains the test data (type of motor, angles to test, the resistance of the machine phase, external resistance). Then, the management software sends the command to the DSP calibrate the encoder position in relation to the rotor position. This is done by unlocking the magnetic brake and triggering the phase being tested. Thus, the rotor pole aligns with the stator and this position is taken as the zero position. After this, the desired position is sent to the DSP which positions the rotor shaft in the test position and sends a confirmation to the LabView.

With the confirmation of the rotor in the desired position, the oscilloscope is configured and should wait for the external trigger to capture the data. Thereafter, the DSP sends the pulse to the oscilloscope trigger and then triggers the phase. The data read in the oscilloscope are obtained via Ethernet. Thus, the flow is calculated using Eq.(1) and then the graphics

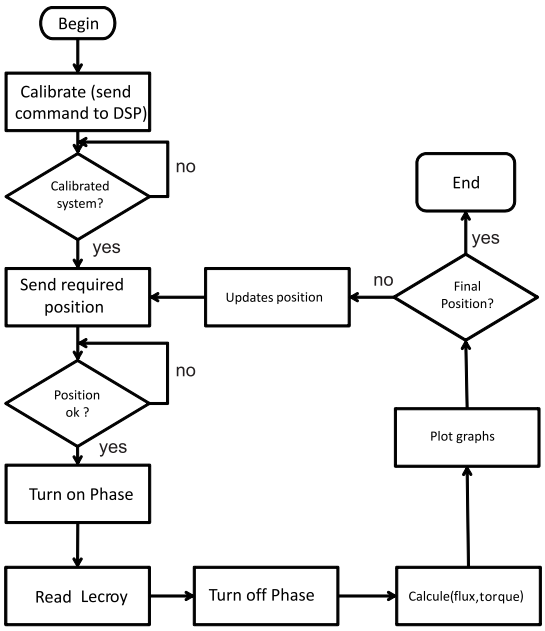

FIGURE 3. Flowchart of the test management software.

$\Phi(I, \theta)$ are plotted. The system repeats the procedure until the final position of the test. Finally, the data curves $\Phi(I, \theta)$ are obtained.

Fig.4 shows the assembled system, wherein an industrial reluctance machine was subjected to test for obtaining the magnetization curves. With the initial data provided by the machine manufacturer (in Appendix), it was possible to determine what would be the required value of the constant current source, considering the machine maximum current during the test. To apply a higher voltage, an external resistor was added in series with the winding under test. With a precision multimeter (Kethey® 2700) a test with four probes was performed and the winding resistance was determined.

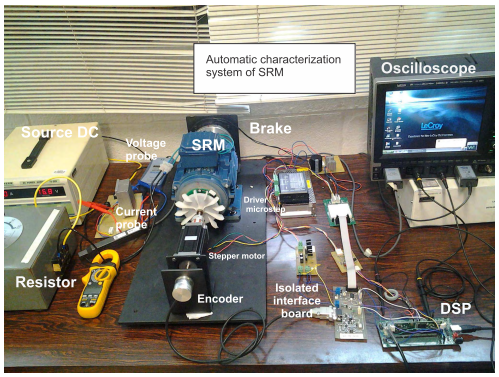

FIGURE 4. Experimental setup designed to test.

The determination of this value is of fundamental importance to ensure the test accuracy.

The experiment was performed from the aligned position until the misaligned position, which in the engine 12/8 corresponds to 22.5° using a fixed step of 2.5°, obtaining 10 experimental magnetization curves for the motor under test.

IV. SRM MATHEMATICAL MODEL

By Eq.(1) the SRM electrical circuit can be modeled as shown in Fig. 5. The equation of the mechanical model is given by Eq.(2) and, as discussed above, the electromagnetic torque is a function of current and position. From Fig.5 it is observed that to perform the mathematical model for SRM simulation, knowing the points $I(\Phi, \theta)$ and points $T(I, \theta)$ is required. From the experimental magnetization curves, lookup tables $I(\Phi, \theta)$ and $T(I, \theta)$ are obtained by mathematical processing. The currents in the stator phases are nonlinear functions $I(\phi, \theta)$ that can be calculated by the magnetization curves $\Phi(I, \theta)$.

$$T_m = T_{emag} - Bw - J\frac{dw}{dt} \tag{2}$$

In [33] and [34] fuzzy logic or intelligent neural networks are used to calculate the magnetic characteristics and to model the SRM. Another way is to obtain analytical equations that relate $I(\Phi, \theta)$ from experimental trials data. Analytical models highlight the methods used by [35], in which Fourier series expansion is used to represent the necessary equations to simulate the SRM.

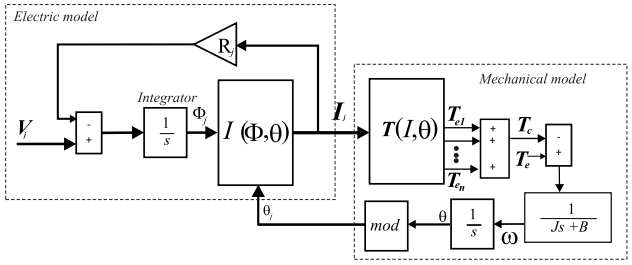

FIGURE 5. SRM phase model.

The use of lookup tables $I(\Phi, \theta)$ and $T(I, \theta)$ allows faster simulations than in the other aforementioned forms. However, to obtain an accurate model, countless magnetization curves are required, wich is infeasible to be performed experimentally, such as obtaining magnetization curves for 200 positions or more. However, with the mathematical processing of test data, it is possible to obtain intermediate curves from the experimental ones.

V. PROCESSING OF DATA OBTAINED IN TESTS

The methodology performed in this article consists in processing the data obtained in magnetizing tests to obtain the necessary lookup tables. Initially, it is assumed to have tables with $N_{points} \times N_{points}$ to get table $I(\Phi, \theta)$. Flux is ranging from 0 to the maximum flux Φ_{max} (obtained from aligned position) in steps of $\frac{\Phi_{max}}{N_{points}}$, the position is ranging from 0° to 45° in steps of $\frac{45°}{N_{points}}$.

With experimental curves $\Phi(I, \theta)$ for the known positions, polynomial fits are used on these data to obtain the functions given in Eq.(3). Coefficients are shown in Table 2. The result of the polynomial fits is very precise once, for each position, it has ten thousand experimental points (I, Φ).

$$\Phi(i)_{\theta=n|_0^{22.5}} = p_0^n + p_1^n i + p_2^n i^2 + p_3^n i^3 + p_4^n i^4 + p_5^n i^5 + p_6^n i^6 \tag{3}$$

Fig.6 shows the curves obtained from the regression. From Eq.(3), for currents from 0 to I_{max} in steps of $\frac{I_{max}}{N_{points}}$, one has the table b of Fig.7 with experimental angles and tabulated currents. With these data it is possible to obtain the points $(\theta, \Phi)|_{I=constant}$, i.e., how the flux behaves varying rotor position for a constant current. For each current there are 10 points (θ, Φ). Therefore, it is important to have a high number of experimental curves for various positions in order to achieve consistent adjustments.

The profile of the magnetic flux in an SRM for a constant current behavior is so that, for the aligned position $(\theta = 0)$, the reluctance of the magnetic circuit is minimal and, therefore, magnetic flux is maximum. As the rotor poles aligns with stator poles, the reluctance increases and the magnetic flux decreases, fact that occurs until the position of the

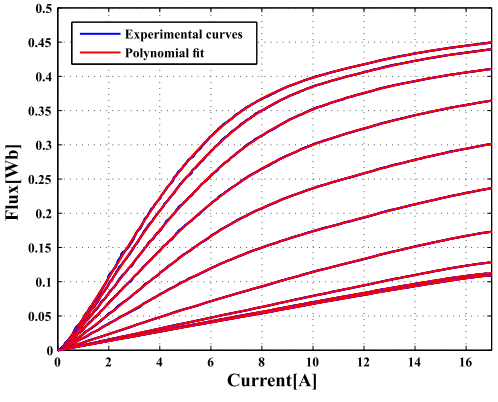

FIGURE 6. Polynomial magnetization curves.

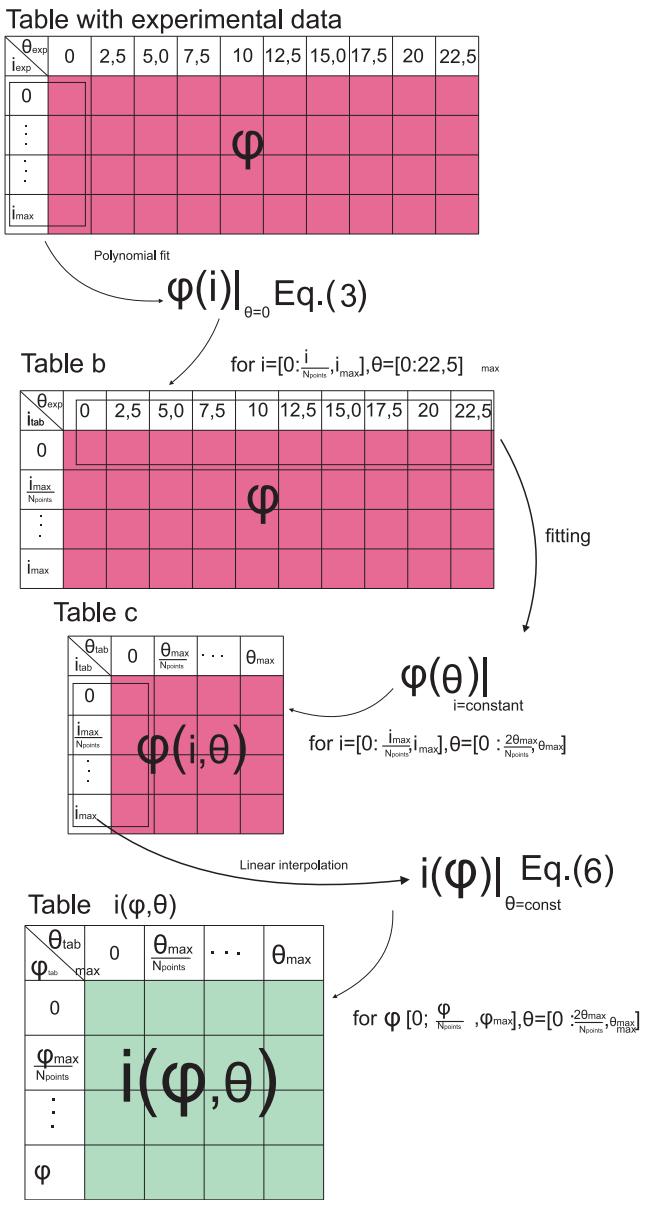

FIGURE 7. Procedure performed to obtain $I(\Phi, \theta)$.

maximum poles misalignment ($\theta = 22.5$) in an SRM 12/8 poles. However, if the rotor width and stator poles are different, in the next total misalignment position the magnetic flux can remain constant. Errors in experimental tests may result in differences in magnetic flux next alignment and misaligned of the poles as discussed in [26]. These errors can cause inaccuracies in models obtained from experimental data.

Attainment of functions can be compromised by the use of not robust regressions that lead to errors arising from experimental tests. Hence, many types of regressions (polynomial, linear, cubic spline) were compared and the use of smoothing spline techniques is proposed to get curves $(\theta, \Phi)|_{I=constant}$ consistent with the operation of SRM.

Polynomial fits may present accentuated oscillations mainly within the limits of the interpolation interval [36].

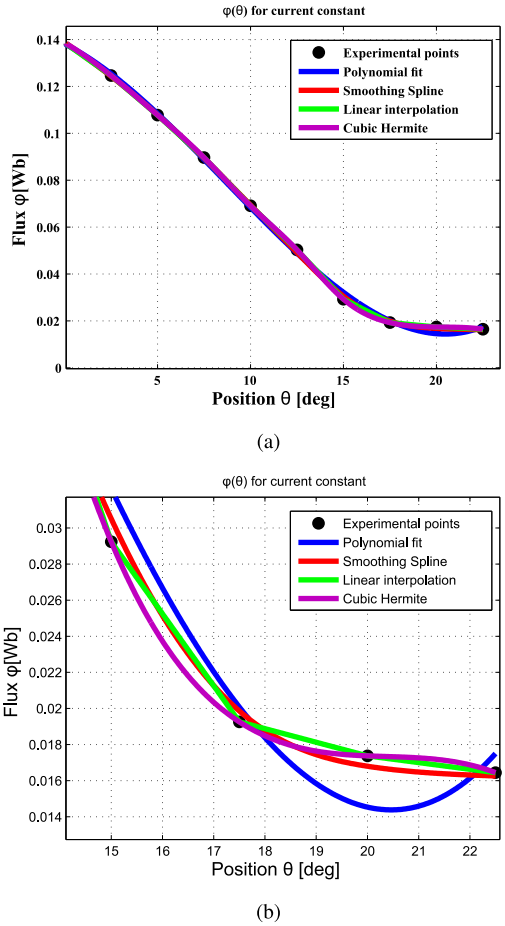

FIGURE 8. a) Flux for different position with current constant, b) Zoom.

This may be accentuated due to the variation characteristic profile of the flux for a specific current in a position close to the alignment and misalignment of SRM poles. As it can be seen in Fig.8(a) and in detail in Fig.8(b), polynomial interpolation showed inconsistent oscillations with the reality of the variation profile of the flux in an SRM, wherein from the aligned position the flux decreases smoothly to the misaligned position.

Piecewise linear interpolation is a simple and easy technique. The idea is to connect straight lines between data points. This technique was used for modeling SRM in [2]. However, in this case when the data point was small, the Piecewise linear interpolation implies in not smooth curves [37].

For smooth interpolation, the use of cubic spline used in [26] and [38] was tested, which determines cubic polynomials that fit smoothly, allowing interpolations with less variation. However, the accuracy on the cubic spline depends strongly on the amount of input data and the fact that the curve obtained passes through all the interpolating points and means that this method is not robust to errors in the experimental data, especially next to the alignment/misaligned positions of the pole regions.

Thus, in this article it is proposed to use more robust and smoother technique known as smoothing spline of curves. Smoothing spline minimizes Eq.(4), that represents the sum of square errors (first term) and the second term represents the roughness turning the curve interpolation smoother [37]. Parameter p defines the smoothing spline. As discussed in [39], an interesting value for the parameter p is given by Eq.(5), where h is the average spacing between the points.

$$p\sum_{i}(y_i - s(x_i))^2 + (1-p)\int(\frac{d^2s}{dx^2})^2dx \tag{4}$$

$$p = \frac{1}{1+\frac{h^3}{6}} \tag{5}$$

In Fig.8(a) it is observed the smoothness obtained using smoothing splines.

With the curves obtained from the current ranging from 0 to I_{max} in steps of $\frac{I_{max}}{N_{points}}$ and for all positions, table c in Fig. 7 is obtained.

As previously discussed, to perform computational model, the current in function of flux and position is required. Through table c in Fig.7, for each position there are points (Φ, I). With these points, by a linear interpolation, one has the functions $I(\Phi)$ in Eq.(6). In this case, linear interpolation was used because it allows extrapolating the current value of the test, if necessary. It occurs unlike the polynomial fit, in which when values surplus the set points, it presents a high error.

$$I(\Phi)_{\theta=const} = i_0 + (i_1 - i_0)\frac{\Phi - \Phi_0}{\Phi_{(1)} - \Phi_{(0)}} \tag{6}$$

With (6) for flux from 0 to Φ_{max} (while Φ_{max}/N_{points}), table $I(\Phi, \theta)$ in Fig. 7 is obtained. This table is reflected since the SRM polar angle is 45 degrees and the test was performed from 0 to 22.5. By the end, the required table is obtained to be used in the simulation model.

Through data from table b from Fig. 7, using the trapezoidal method to calculate the integral, coenergy is estimated by Eq.(7).

$$W_n^{'}(i)|_{\theta=const} = trapz(i[1:n], \Phi[1:n])|_2^{N_{points}} \tag{7}$$

For a constant current, one has the pairs of points (w, θ), which make possible to calculate the electromagnetic torque for a given current as a function of position using Eq.(8).

$$T = \frac{180}{\pi}\frac{(W_n^{'} - W_{n-1}^{'})}{(\theta_n - \theta_{n-1})}|_{n=2}^{Npontos} \tag{8}$$

Figs.9 and 10 present the inductance and electromagnetic torque, respectively, as a function of position and current obtained using the described interpolation methods, to obtain the functions $(\theta, \Phi)|_{I=constante}$. It is observed that the use of polynomial interpolation, linear interpolation and cubic spline in the calculation of the functions resulted in mistakes of variations in torque and inductance profile not consistent with the SRM operation. These oscillations can cause problems in projects that require accurate models as for decrease in torque oscillations and position estimation. The smoothing splines technique showed the best results that are consistent with the real SRM characteristics.

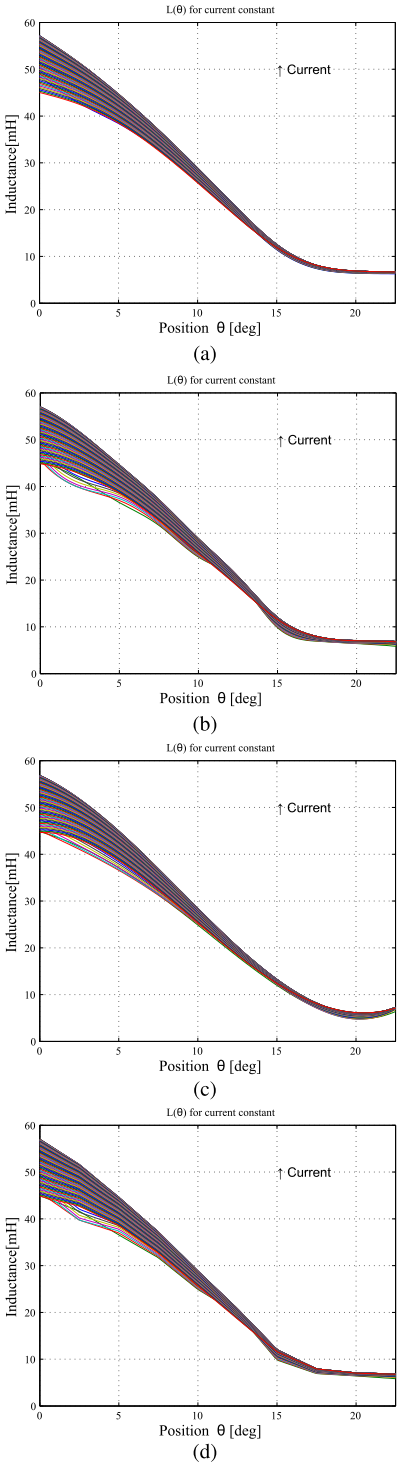

FIGURE 9. Inductance for current and position a) Smoothing spline, b) Hermite cubic, c) Polynomial fit, d)Linear interpolation.

VI. OBTAINED MODEL SIMULATION

With lookup tables data $I(\Phi, \theta)$ and $T(I, \theta)$, the SRM model (Fig. 5) was implemented in Simulink®. To verify

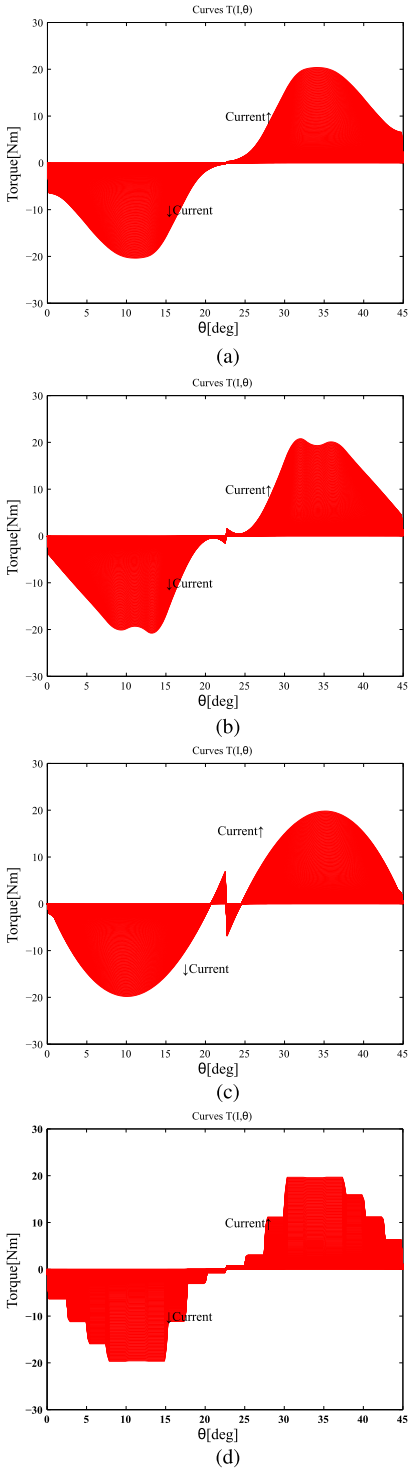

FIGURE 10. Torque for current and position a) Smoothing spline, b) Hermite cubic, c) Polynomial fit, d)Linear interpolation.

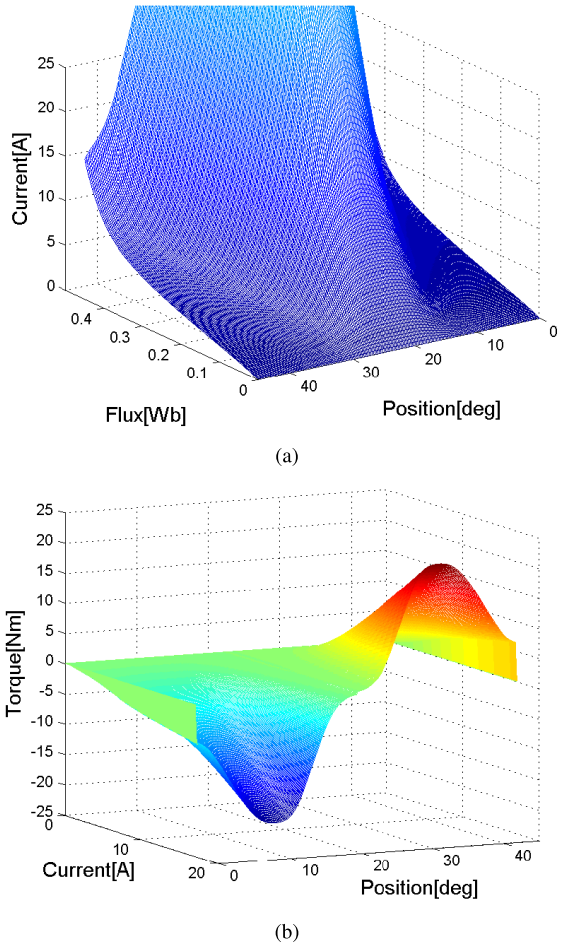

FIGURE 11. Lookup tables data a) $I(\Phi, \theta)$, b) $T(I, \theta)$.

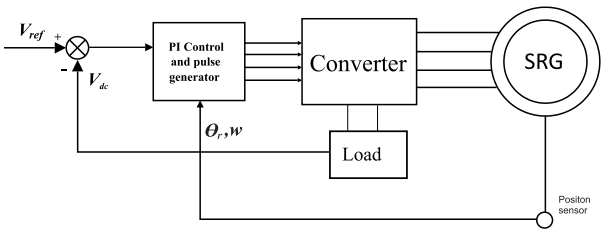

FIGURE 12. Simulated control system of SRG.

the developed model operation, a control system for SRM operating as a generator was simulated. Fig. 12 shows the diagram of the bus voltage control system. The switched reluctance generator (SRG) operated at a constant speed equals to 1200 r/min. The SRG feeds resistive loads and the control is responsible for maintaining the bus voltage on the reference value V_{ref}. A PI controller processes the error between the reference voltage and the bus voltage and acts on the turn off angle, controlling the SRG level of magnetization to maintain a constant DC level.

Figs.11(a) and 11(b) show respectively the data of table $I(\Phi, \theta)$ and the table of torque $T(I, \theta)$.

VII. EXPERIMENTAL SETUP

To verify the precision and efficiency of the model obtained, an experimental setup was assembled in the same condition of the simulation test. DSP TMS320F28335 was used to control the DC voltage. The controller of the simulations was discretized (sample time of 40kHz) and computed in the DSP.

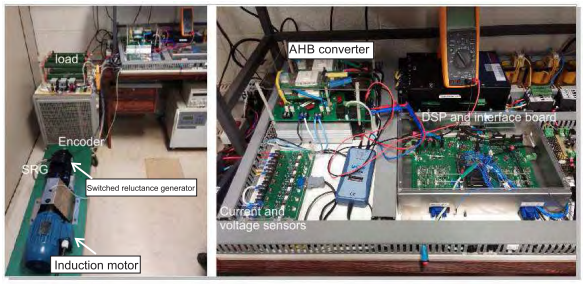

FIGURE 13. Experimental setup photography.

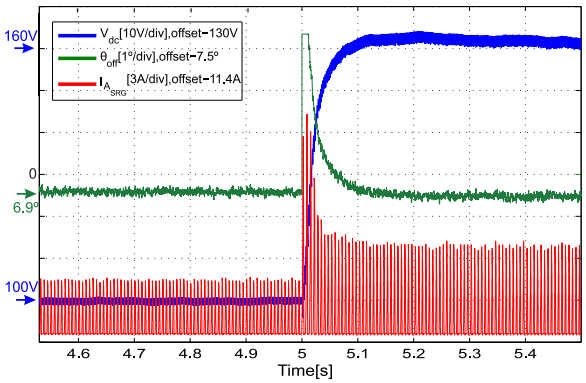

FIGURE 14. Simulation results.

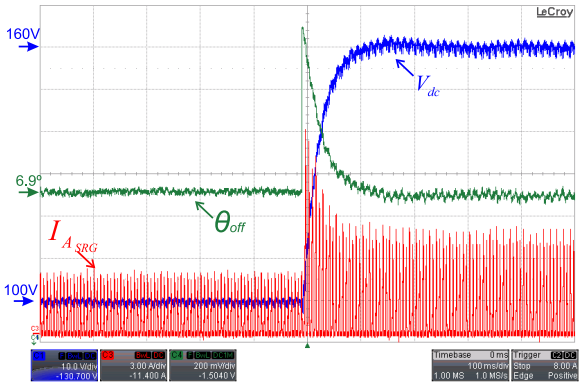

FIGURE 15. Experimental results.

An Asymmetric Half Bridge (AHB) converter was used to drive the phases of the generator. An induction motor (IM) driven by an inverter was used as the prime mover. By an absolute encoder, the DSP obtains the position of the SRG rotor. A pulse generator drives the phase of the motor in the correct moment. Fig.13 shows the experimental systems in the laboratory.

VIII. SIMULATION AND EXPERIMENTAL RESULTS

Simulation was set to start with a load of 180 Ω and $V_{ref} = 100\ V$. In 5s of simulation V_{ref} is set on 160 V. The DC bus voltage is shown in Fig.12. For SRG operating in a self excited mode, it is necessary an initial magnetization, which is, in this case, provided by the capacitor of DC bus. It is observed that the control acted in θ_{off} angle and increased the

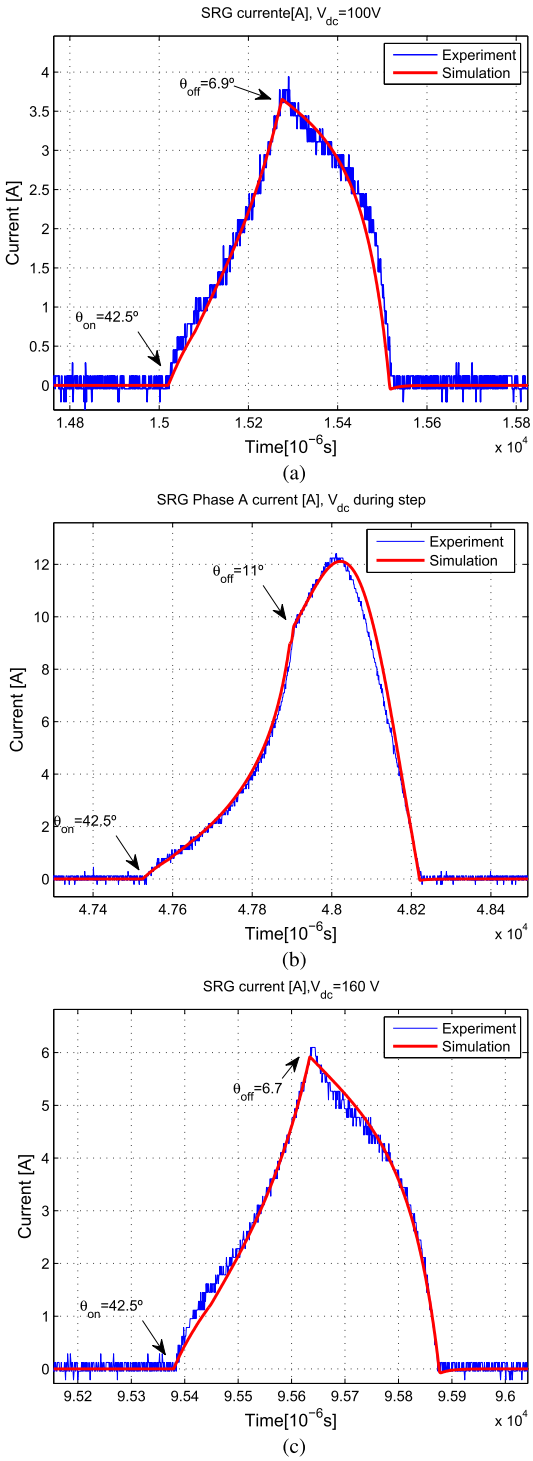

FIGURE 16. Simulated and experimental SRG currents a) $V_{dc} = 100V$, b) Step in V_{dc}, c) $V_{dc} = 160V$.

SRG excitement to supply the energy to be generated, keeping the DC bus voltage at the reference value. Several techniques can be applied to control the DC bus voltage as presented by [40]. The DC link capacitor (2250 uF)is responsible for filtering the voltage ripple. Fig.14 shows the results of the control, DC bus voltage, θ_{off} angle and SRG current, whereat it is possible to notice the control is operating efficiently.

The results of the experimental test in Fig.15 are very similar to the results of simulations in Fig.14.

The electric currents of the experiment and simulation test are compared in Fig.16. To evaluate the accuracy of the obtained model, statistical parameters were calculated, such as the root mean square error (RMSE), mean absolute error (MAE), sum of squares error (SSE) and R-square (R^2). RMSE and MAE of relative errors at current SRG are defined in (9) and (12).

$$RMSE = \sqrt{\frac{1}{n}\sum_{j=1}^{n}(e_{avg} - e_j)^2} \tag{9}$$

$$e_j = \left|I_{exp} - I_{sim}\right| / I_{exp} x 100\% \tag{10}$$

$$e_{avg} = \frac{1}{n}\sum_{j=1}^{n} e_j \tag{11}$$

$$MAE = mean(e_j) \tag{12}$$

Where I_{exp} and I_{sim} are the measured and simulated SRG current, n is the number of data points, e_j and e_{avg} are relative errors and their average value, respectively.

Table 1 shows the results of statistic analysis of current in time of Fig. 16. It is seen that the model obtained by the developed instrumentation using the smoothing splines describes accurately the nonlinear magnetic characteristics of the switched reluctance motors.

TABLE 1. Statistics goodness-of-fit parametric.

T_{srm}	error	MAE	R^2	RMSE	SSE
100V	0.21A	6.80%	0.974	0.1446	8.94
160V	0.017A	4.99%	0.9888	0.1572	10.57
Step	0.28A	5.73%	0.9877	0.4023	85.46

TABLE 2. Coeficientes polynomial fits.

θ	p0	p1	p2	p3	p4	p5	p6
0.0^o	-6.51e^{-9}	3.05e-7	-5.78e-6	5.37e-5	-2.49e-4	7.28e-3	-3.29e-4
2.5^o	-5.06e-9	1.94e-7	-2.87e-6	2.02e-5	-7.97e-5	7.23e-3	-1.89e-4
5.0^o	-7.56e-9	3.04e-7	-4.56e-6	3.00e-5	-7.91e-5	8.01e-3	-2.92e-4
7.5^o	6.81e-9	-4.70e-7	1.18e-5	-1.40e-4	6.61e-4	1.10e-2	-1.83e-4
10.0^o	8.89e-9	-1.03e-6	3.64e-5	-5.39e-4	2.89e-3	1.54e-2	-2.63e-4
12.5^o	-8.81e-9	-3.85e-7	3.29e-5	-6.46e-4	3.89e-3	2.13e-2	-1.30e-3
15.0^o	-1.52e-8	-1.23e-7	3.16e-5	-7.03e-4	4.22e-3	2.94e-2	-2.04e-3
17.5^o	-6.87e-9	-6.83e-7	4.72e-5	-9.12e-4	5.11e-3	3.58e-2	-2.69e-3
20.0^o	2.72e-8	-3.01e-6	1.06e-4	-1.57e-3	7.77e-3	4.00e-2	-3.91e-3
22.5^o	9.38e-8	-6.95e-6	1.94e-4	-2.45e-3	1.10e-2	4.06e-2	-3.01e-3

IX. CONCLUSION

The system for SRM electromagnetic characterization developed in this work allowed to obtain automatically and accurately the magnetization curves for an SRM 12/8. With the experimental curves, it was possible to have a consistent nonlinear behavior of the SRM that allow simulations in order to make technical control and decrease the oscillation of torque through simulation models. It was observed that the use of the smoothing splines technique in the data processing allowed to obtain an accurate model consistent with the true operation of the SRM. Simulations of a voltage control and its experimental implementation were performed. The results were quite similar, confirming the accuracy and high fidelity of the obtained model.

APPENDIX

Parameters of Switched reluctance machine: $P_n = 1.5kW$; $V_n = 220V$; $w_n = 1500\ r/min$; $\frac{N_s}{N_r} = \frac{12}{8}$; $R_s = 1\ \Omega$; $I_{max} = 18A$;

REFERENCES

[1] R. Krishnan, *Switched Reluctance Motor Drives: Modeling, Simulation, Analysis, Design, and Applications*. Boca Rsaton, FL, USA: CRC Press, 2001.

[2] T. J. E. Miller, *Electronic Control of Switched Reluctance Machines* (Newnes Power Engineering Series). New York, NY, USA: Elsevier, 2001.

[3] S. Sezen, E. Karakas, K. Yilmaz, and M. Ayaz, "Finite element modeling and control of a high-power SRM for hybrid electric vehicle," *Simul. Model. Pract. Theory*, vol. 62, pp. 49–67, Mar. 2016.

[4] K. Kiyota, T. Kakishima, and A. Chiba, "Comparison of test result and design stage prediction of switched reluctance motor competitive with 60-kW rare-Earth PM motor," *IEEE Trans. Ind. Electron.*, vol. 61, no. 10, pp. 5712–5721, Oct. 2014.

[5] R. Cardenas, R. Pena, M. Perez, J. C. G. Asher, and P. Wheeler, "Control of a switched reluctance generator for variable-speed wind energy applications," *IEEE Trans. Energy Convers.*, vol. 20, no. 4, pp. 691–703, Dec. 2005.

[6] H. Chen and J. J. Gu, "Implementation of the three-phase switched reluctance machine system for motors and generators," *IEEE/ASME Trans. Mechatronics*, vol. 15, no. 3, pp. 421–432, Jun. 2010.

[7] D. Wu, J. Shi, Z. Zhu, and X. Liu, "Electromagnetic performance of novel synchronous machines with permanent magnets in stator yoke," *IEEE Trans. Magn.*, vol. 50, no. 9, Sep. 2014, Art. no. 8102009.

[8] Y. Hu, X. Song, W. Cao, and B. Ji, "New SR drive with integrated charging capacity for plug-in hybrid electric vehicles (PHEVs)," *IEEE Trans. Ind. Electron.*, vol. 61, no. 10, pp. 5722–5731, Oct. 2014.

[9] C. Capovilla, I. Santana, A. Filho, T. Barros, and E. Ruppert, "Performance of a direct power control system using coded wireless OFDM power reference transmissions for switched reluctance aerogenerators in a smart grid scenario," *IEEE Trans. Ind. Electron.*, vol. 62, no. 1, pp. 52–61, Jan. 2015.

[10] T. A. S. Barros and E. R. Filho, "Direct power control for switched reluctance. Generator in wind energy," *IEEE Latin America Trans.*, vol. 13, no. 1, pp. 123–128, Jan. 2015.

[11] Y.-T. Chang and K. Cheng, "Sensorless position estimation of switched reluctance motor at startup using quadratic polynomial regression," *IET Electr. Power Appl.*, vol. 7, no. 7, pp. 618–626, Aug. 2013.

[12] X. She, A. Q. Huang, F. Wang, and R. Burgos, "Wind energy system with integrated functions of active power transfer, reactive power compensation, and voltage conversion," *IEEE Trans. Ind. Electron.*, vol. 60, no. 10, pp. 4512–4524, Oct. 2013.

[13] M. Rafiq, S.-Ur Rehman, F.-Ur Rehman, Q. R. Butt, and I. Awan, "A second order sliding mode control design of a switched reluctance motor using super twisting algorithm," *Simul. Model. Pract. Theory*, vol. 25, pp. 106–117, Jun. 2012. [Online]. Available: http://www.sciencedirect.com/science/article/pii/S1569190X12000342

[14] W. Ding and D. Liang, "A fast analytical model for an integrated switched reluctance starter/generator," *IEEE Trans. Energy Convers.*, vol. 25, no. 4, pp. 948–956, Dec. 2010.

[15] J. Cai, Z. Deng, and R. Hu, "Position signal faults diagnosis and control for switched reluctance motor," *IEEE Trans. Magn.*, vol. 50, no. 9, Sep. 2014, Art. no. 8201811.

[16] J. Corda and S. Jamil, "Experimental determination of equivalent-circuit parameters of a tubular switched reluctance machine with solid-steel magnetic core," *IEEE Trans. Ind. Electron.*, vol. 57, no. 1, pp. 304–310, Jan. 2010.

[17] B. Parreira, S. Rafael, A. J. Pires, and P. J. C. Branco, "Obtaining the magnetic characteristics of an 8/6 switched reluctance machine: From FEM analysis to the experimental tests," *IEEE Trans. Ind. Electron.*, vol. 52, no. 6, pp. 1635–1643, Dec. 2005.

[18] P. Zhang, P. Cassani, and S. Williamson, "An accurate inductance profile measurement technique for switched reluctance machines," *IEEE Trans. Ind. Electron.*, vol. 57, no. 9, pp. 2972–2979, Sep. 2010.
[19] S. Song, M. Zhang, and L. Ge, "A new fast method for obtaining flux-linkage characteristics of srm," *IEEE Trans. Ind. Electron.*, vol. 62, no. 7, pp. 4105–4117, Jul. 2015.
[20] L. Shen, J. Wu, S. Yang, and X. Huang, "Fast flux linkage measurement for switched reluctance motors excluding rotor clamping devices and position sensors," *IEEE Trans. Instrum. Meas.*, vol. 62, no. 1, pp. 185–191, Jan. 2013.
[21] V. Nasirian, S. Kaboli, A. Davoudi, and S. Moayedi, "High-fidelity magnetic characterization and analytical model development for switched reluctance machines," *IEEE Trans. Magn.*, vol. 49, no. 4, pp. 1505–1515, Apr. 2013.
[22] S.-C. Wang, "An fully-automated measurement system for identifying magnetization characteristics of switched reluctance motors," *Measurement*, vol. 45, no. 5, pp. 1226–1238, 2012.
[23] S.-H. Mao and M.-C. Tsai, "An analysis of the optimum operating point for a switched reluctance motor," *J. Magn. Magn. Mater.*, vol. 282, pp. 53–56, Nov. 2004.
[24] X. D. Xue, K. W. E. Cheng, and S. L. Ho, "A self-training numerical method to calculate the magnetic characteristics for switched reluctance motor drives," *IEEE Trans. Magn.*, vol. 40, no. 2, pp. 734–737, Mar. 2004.
[25] X. D. Xue, K. W. E. Cheng, S. L. Ho, and K. F. Kwok, "Trigonometry-based numerical method to compute nonlinear magnetic characteristics in switched reluctance motors," *IEEE Trans. Magn.*, vol. 43, no. 4, pp. 1845–1848, Apr. 2007.
[26] X. D. Xue, K. W. E. Cheng, and S. L. Ho, "Simulation of switched reluctance motor drives using two-dimensional bicubic spline," *IEEE Trans. Energy Convers.*, vol. 17, no. 4, pp. 471–477, Dec. 2002.
[27] B. Ganji, J. Faiz, K. Kasper, C. Carstensen, and R. De Doncker, "Core loss model based on finite-element method for switched reluctance motors," *IET Electr. Power Appl.*, vol. 4, no. 7, pp. 569–577, Aug. 2010.
[28] J. Zhang, H. Zhang, R. Gao, and L. Wang, "Control simulation studies for switched reluctance motor system based on finite element model," in *Proc. 4th IET Conf. Power Electron., Mach. Drives (PEMD)*, Apr. 2008, pp. 169–173.
[29] F. L. M. dos Santos, J. Anthonis, F. Naclerio, J. J. C. Gyselinck, H. Van der Auweraer, and L. C. S. Goes, "Multiphysics NVH modeling: Simulation of a switched reluctance motor for an electric vehicle," *IEEE Trans. Ind. Electron.*, vol. 61, no. 1, pp. 469–476, Jan. 2014.
[30] D. Torrey, X.-M. Niu, and E. Unkauf, "Analytical modelling of variable-reluctance machine magnetisation characteristics," *IEE Proc. Electr. Power Appl.*, vol. 142, no. 1, pp. 14–22, Jan. 1995.
[31] J. Sun, Q. Zhan, Y. Guo, and J. Zhu, "Back propagation neural network applied to modeling of switched reluctance motor," in *Proc. 12th Biennial IEEE Conf. Electromagn. Field Comput.*, Apr./May 2006, p. 151.
[32] V. Oliveira, R. Pontes, D. Oliveira, R. C. de Almeida, and W. da Silva, "Investigation the design of a RSRM through the analysis of the finite elements with experimental validation," in *Proc. 10th IEEE/IAS Int. Conf. Ind. Appl. (INDUSCON)*, Nov. 2012, pp. 1–6.
[33] W. Ding and D. Liang, "Modeling of a 6/4 switched reluctance motor using adaptive neural fuzzy inference system," *IEEE Trans. Magn.*, vol. 44, no. 7, pp. 1796–1804, Jul. 2008.
[34] T. Lachman, T. R. Mohamad, and C. H. Fong, "Nonlinear modelling of switched reluctance motors using artificial intelligence techniques," *IEE Proc.-Electr. Power Appl.*, vol. 151, no. 1, pp. 53–60, Jan. 2004.
[35] D. Andrade and R. Krishnan, "Characterization of switched reluctance machines using fourier series approach," in *Proc. 36th IAS Annu. Meeting Conf. Rec. IEEE Ind. Appl. Conf.*, vol. 1. Sep. 2001, pp. 48–54.
[36] D. Kahaner, C. Moler, and S. Nash, *Numerical Methods and Software*. Englewood Cliffs, NJ, USA: Prentice-Hall, 1988.
[37] C. de Boor, *A Practical Guide to Splines* (Applied Mathematical Sciences). New York, NY, USA: Springer, 2001.
[38] J. C. Moreira, "Torque ripple minimization in switched reluctance motors via bi-cubic spline interpolation," in *Proc. Rec., 23rd Annu. IEEE Power Electron. Specialists Conf. (PESC)*, vol. 2. Jun. 1992, pp. 851–856.
[39] C. Moler, *Numerical Computing With MATLAB*. Philadelphia, PA, USA: SIAM, 2004.
[40] A. Silveira, D. Andrade, A. Fleury, L. Gomes, C. Bissochi, and R. Dias, "Voltage control in starter/generator SRM based systems," in *Proc. IEEE Energy Convers. Congr. Expo. (ECCE)*, Sep. 2009, pp. 2460–2465.

TÁRCIO ANDRÉ DOS SANTOS BARROS (S'14–M'17) received the bachelor's degree in electrical engineering from the Federal University of Vale do São Francisco, Petrolina, Brazil, in 2010, and the M.S. and Ph.D. degrees from the University of Campinas, Campinas, Brazil, in 2012 and 2015, respectively. From 2016 to 2017, he was a Researcher with the University of Campinas, under the FAPESP Post-Doctoral Program. He is currently a Professor with the University of Campinas. He involves in the areas of electrical machines, power electronics, and electrical drives. His research interests include machine drives, switched reluctance machines, doubly fed induction generators, and solar energy. He is a member of the PELS and the Brazilian Society of Power Electronics.

PEDRO JOSÉ DOS SANTOS NETO received the bachelor's degree in electrical engineering from the Federal University of Vale do São Francisco, Petrolina-PE, Brazil, in 2016, and the M.S. degree from the University of Campinas (UNICAMP), Campinas-SP, Brazil, in 2017. He is currently pursuing the Ph.D. degree from UNICAMP. He involves in the areas of electrical machines, power electronics, and electrical drives. His research interests include renewable energy, distributed generation, DC microgrids, switched reluctance machines, and permanent magnet synchronous generator.

MARCELO VINICIUS DE PAULA received the B.S. degree in electrical engineering from the Federal University of Goiás, Goiânia, Brazil, in 2016. He is currently pursuing the M.S. degree with the University of Campinas, Campinas, Brazil, under the CNPq Scholarship Program. He involves in the areas of electric machines and drives, power electronics and electric vehicles. His research interests are torque ripple minimization, switched reluctance machine drives, electric vehicles, and renewable energy.

ADSON BEZERRA MOREIRA received the B.Sc. degree in electrical engineering from the Federal University of Ceará in 2003, and the M.Sc. and Ph.D. degrees in electrical engineering from the University of Campinas, Campinas, Brazil, in 2006 and 2018, respectively. Since 2008, he has been with the Federal University of Ceará, Sobral, Brazil, where he is currently an Assistant Professor. His research interests include energy efficiency, power quality, electric machine drives, and power generation.

PAULO SERGIO NASCIMENTO FILHO graduated in electrical engineering and received the master's degree in electrical engineering from the Federal University of Pará, in 2009 and 2011, respectively, where he researched the control of dynamical systems applied in electric power generation systems with Highlight for speed controllers of hydraulic turbines and thermal turbines, voltage regulators of synchronous generators and power stabilizers system, and the Ph.D. degree in electrical engineering from the State University of Campinas with a scholarship from CNPq in 2017, where he researches advanced control strategies and power electronics applied to power systems and distributed generation.

ERNESTO RUPPERT FILHO received the B.S. degree in electrical engineering and the M.S. and Ph.D. degrees from the University of Campinas (UNICAMP), Campinas, Brazil, in 1971, 1974, and 1983, respectively. From 1972 to 1978, he was with the Electrical and Computer Engineering School, UNICAMP, as an Assistant Professor of electromechanical energy conversion. From 1979 to 1983, he was with General Electric, Brazil, as an Application Engineer dedicated to large motors and generators, and designing large induction and synchronous motors. From 1983 to 1989, he was with Vigesa Heavy Equipment, Brazil, designing very large hydrogenerators and also performing commissioning tests on hydropower plants in Brazil. He is currently a Full Professor with the Electrical and Computer Engineering School, UNICAMP, researching and teaching in the areas of electrical machines, power electronics, drives, and electrical power systems.